

# Transition to the ultimate regime in a stochastic model for thermal convection with internal sources

Marten Klein<sup>1\*</sup>, Heiko Schmidt<sup>1</sup> & Alan R. Kerstein<sup>2</sup>

<sup>1</sup>Numerical Fluid and Gas Dynamics, Brandenburg University of Technology (BTU) Cottbus-Senftenberg, Germany

<sup>2</sup>Consultant, Danville, CA, USA

\* Contact: [marten.klein@b-tu.de](mailto:marten.klein@b-tu.de)

**b-tu**

Brandenburg  
University of Technology  
Cottbus - Senftenberg

## What is turbulent thermal convection with internal sources?

- **Turbulent thermal convection** denotes the chaotic flow in a layer of fluid that is driven by buoyancy forces due to an unstable temperature stratification. The flow becomes turbulent when buoyancy and inertial forces are much larger than viscous forces. This type of flow is encountered in numerous applications that range from technical to atmospheric and astrophysical scales (for an overview, see e.g. [1] and references therein).
- **Internal sources (sinks)** heat (cool) the fluid from within like, for example, by radiation [2] or condensation [3]. The forcing considered in this study is canonical but complementary to fixed temperature and isoflux boundary conditions.

## Main objectives

- Investigation of **turbulent scaling regimes** of the heat transfer in thermal convection with internal sources and sinks.
- **Modeling** using a numerical tool applicable throughout the **relevant parameter space**.
- Capture **transient boundary layers** by utilizing the **one-dimensional turbulence model** [4].

## Model formulation

The **ODT model** aims to **resolve all relevant scales** of a turbulent flow along a notional line-of-sight ('ODT line'). Flow variables are resolved along this line on a dynamically adaptive grid [5]. Instantaneous flow profiles are evolved by **deterministic diffusion** along the ODT domain, and a **stochastic process** that models the effects of turbulent advection, pressure fluctuations, and buoyancy forces that are aligned with the ODT domain ( $z$  coordinate) [4, 6, 7].

- **ODT governing equations** for the Cartesian velocity components  $u_i$  and the temperature  $T$  are

$$\frac{\partial u_i}{\partial t} + \mathcal{E}_i(\alpha) = \nu \frac{\partial^2 u_i}{\partial z^2}, \quad \frac{\partial T}{\partial t} + \mathcal{E}_T = \kappa \frac{\partial^2 T}{\partial z^2} + \frac{Q_{\text{tot}}}{\rho c_p},$$

where  $\nu$  is the kinematic viscosity,  $\rho$  the reference mass density,  $c_p$  the specific heat capacity at constant pressure,  $\kappa = \lambda/(\rho c_p)$  the thermal diffusivity with  $\lambda$  the thermal diffusivity, and  $Q_{\text{tot}}$  the heat sources and sinks.

- **Stochastic terms**  $\mathcal{E}_i$  and  $\mathcal{E}_T$  represent the effects of discrete turbulent **eddy events** in which the **triplet map** models an eddy turnover (**Fig. 1**).
- The **eddy rate**  $\tau^{-1}(\ell_e, z_0; t)$  of a size- $\ell_e$  eddy event at location  $z_0$  at time  $t$  depends on the **total available eddy energy** for the momentary flow state. The eddy rate reads [6, 7]

$$\tau^{-1} = C \sqrt{2 \ell_e^{-2} (E_{\text{kin}} + E_{\text{pot}} - Z E_{\text{vp}})},$$

where  $E_{\text{kin}}$  and  $E_{\text{pot}}$  denote the eddy kinetic and potential energy, respectively, and  $E_{\text{vp}}$  is a viscous penalty energy to suppress eddies below a viscous length scale [4].

- **Fixed ODT model parameters**  $C = 60$ ,  $Z = 220$ , and  $\alpha = 2/3$  are used here. Definitions are identical to [7] but the calibration was performed for canonical Rayleigh-Bénard convection with  $Pr \lesssim 1$  [8].

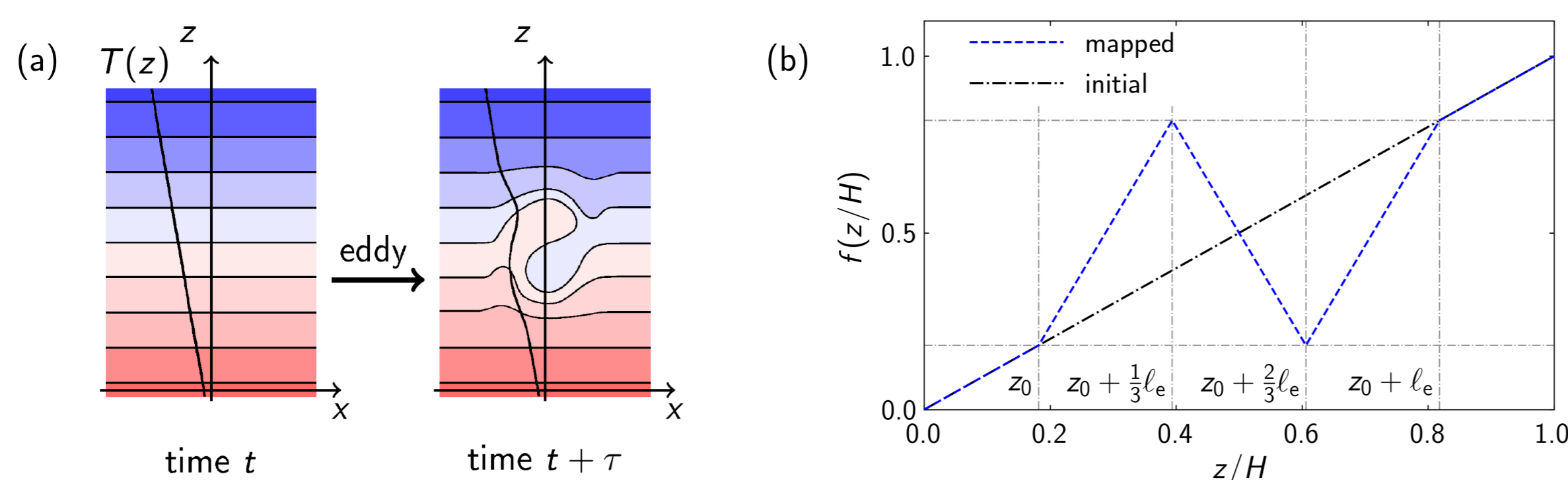


**Figure 1:** (a) Schematic of an eddy turnover. (b) Triplet map for an eddy event that covers the interval  $0.2 \leq z/H \leq 0.8$ .

## Flow configuration and model application

- **Layer of fluid** of height  $H$  for which wall-normal transport is resolved by a vertical ODT line (**Fig. 2**)
- Uniform **constant gravity**  $g = -g e_z$
- **Oberbeck-Boussinesq fluid:** linear equation of state,  $\rho(T) = \rho_0 [1 - \beta(T - T_0)]$ , where  $\beta$  is the thermal expansion coefficient, and subscript 0 denotes reference values
- **Smooth adiabatic no-slip wall** at bottom  $z = 0$  and top  $z = H$
- **Heat sources/sinks:**  $Q_{\text{tot}} = Q(z) - \langle Q \rangle_z$ , where  $Q(z) = (P/\ell) \exp(-z/\ell)$  is the local heating rate,  $-\langle Q \rangle_z$  the spatial mean cooling rate,  $\ell$  a prescribed length scale, and  $P$  the power influx [9].
- The flow is characterized by the **Prandtl**, **Rayleigh**, and **Nusselt number**,

$$Pr = \frac{\nu}{\kappa}, \quad Ra = \frac{g \beta \langle \Delta T \rangle H^3}{\nu \kappa}, \quad Nu = \frac{PH}{\lambda \langle \Delta T \rangle},$$

where  $\Delta T = T|_{z=0} - T|_{z=H/2}$  is a convenient definition of a **wall-bulk temperature difference** with temporal average  $\langle \Delta T \rangle$ . This is similar to [9].

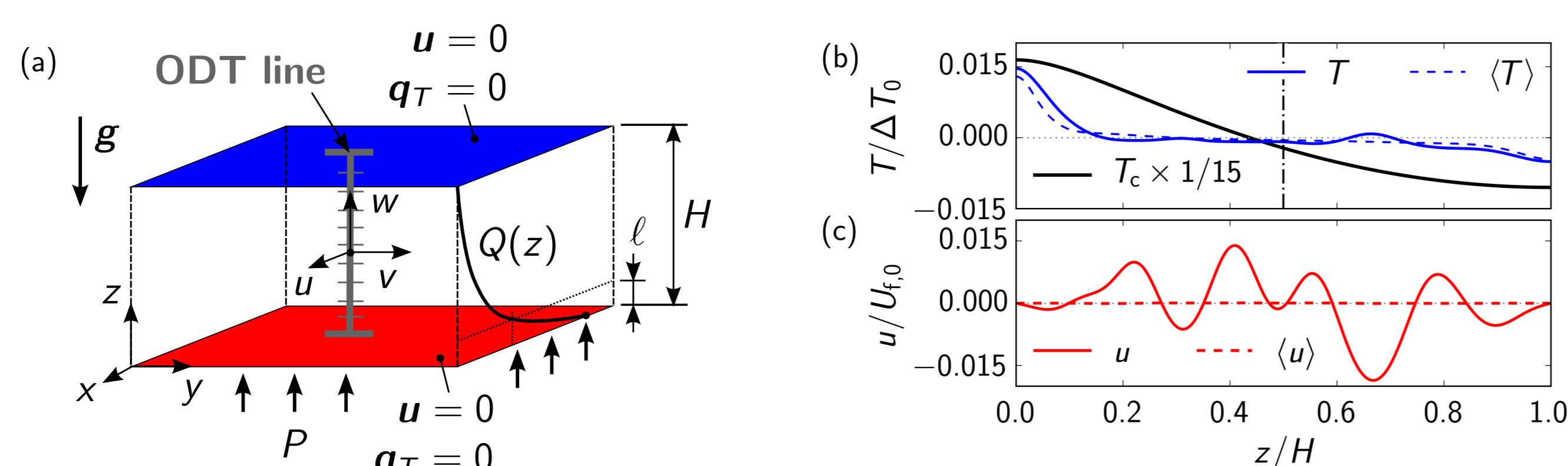


**Figure 2:** (a) Sketch of the set-up. The fluid is heated by the profile  $Q(z)$  with total power influx  $P$  analogous to [9]. (b) Vertical profiles of the instantaneous and temporal-averaged temperature,  $T$  and  $\langle T \rangle$ , respectively.  $T_c$  denotes the purely conductive analytic solution that has been compressed here to fit in the plotting range. (c) Vertical profiles of the instantaneous and temporal-averaged horizontal velocity component  $u$ . Control parameters are  $Pr = 1$ ,  $Ra = 10^8$ , and  $\ell/H = 0.096$ . Reference scales are given by the flux temperature difference  $\Delta T_0 = PH/\lambda$  and the corresponding free-fall velocity  $U_{f,0} = \sqrt{g \beta \Delta T_0 L}$ .

## Scaling regimes of the heat transfer for $Pr = 1$

Grossmann & Lohse [10] showed that effective scalings of the heat transfer result from **bulk and boundary-layer contributions**. For temperature or heat-flux prescribed by boundary conditions, the different contributions develop dynamically and can *not* be individually controlled (unless surface roughness is used which introduces other complications). In the current configuration with internal heat sources/sinks the problem is addressed by introducing the **thermal length scale  $\ell/H$  as additional control parameter** to manipulate the thermal boundary layer.

- **Fig. 3(a)** shows **multiple scalings** of the heat transfer in terms of

$$Nu \sim Ra^p (\ell/H)^q \quad \text{for fixed } Pr = 1.$$

Reference experimental results [9] (black symbols) are shown together with ODT simulation results (color symbols) that exhibit good **qualitative and quantitative agreement**.

- Various **effective scaling laws** (black lines) are shown for comparison:  $p = 1/3$  (Malkus [11]),  $p = 2/7$  (Shraiman & Siggia [12]),  $p = 1/2$  ('ultimate Rayleigh-Bénard' [13]), and  $p \approx 0.55$  (present 'ultimate ODT') scaling. Latter slightly exceeds 'ultimate' (turbulence-only)  $p = 1/2$ , which is a strict upper bound for canonical Rayleigh-Bénard convection [14] but *not* for convection with internal sources, where the maximum is  $p_{\text{max}} = 1$  that has been achieved for laminar rolls [15].

- **Fig. 3(b)** shows **rescaled data**  $Nu/Nu_X$  vs.  $Ra/Ra_X$ , where the subscript 'X' indicates a notional transition point. Following Bouillaut and colleagues [9], we solve for the intersection of the Malkus ( $p = 1/3, q = 0$ ) and the 'ultimate ODT' ( $p \approx 0.55, q = 1$ ) scaling, that is,

$$Nu_X \sim Ra_X^{1/3} \sim (\ell/H) Ra_X^{0.55}.$$

This transformation **collapses the ODT and reference data** equally well.

- **Fig. 3(c)** shows the **scaling exponent  $p$**  vs.  $\ell/H$  for high  $Ra$  numbers. Here,  $p$  was obtained by fitting  $Nu \sim Ra^p$  for a central region of each simulated  $\ell/H$  dataset. A **plateau** is visible on the right. This is the mixing-length ('ultimate') regime for large  $\ell/H$  with  $p \approx 0.55$ . A logarithmic variation of  $p$  can be discerned to the left in the transitional  $\ell/H$  range. The exponent  $p$  seems to level again for very small  $\ell/H$  in between classical values  $p = 2/7$  and  $1/3$ .

- **Conventional and unbiased (log-based) statistics** are used to demonstrate statistical convergence. For the cases simulated, the methods yield **virtually identical results**.

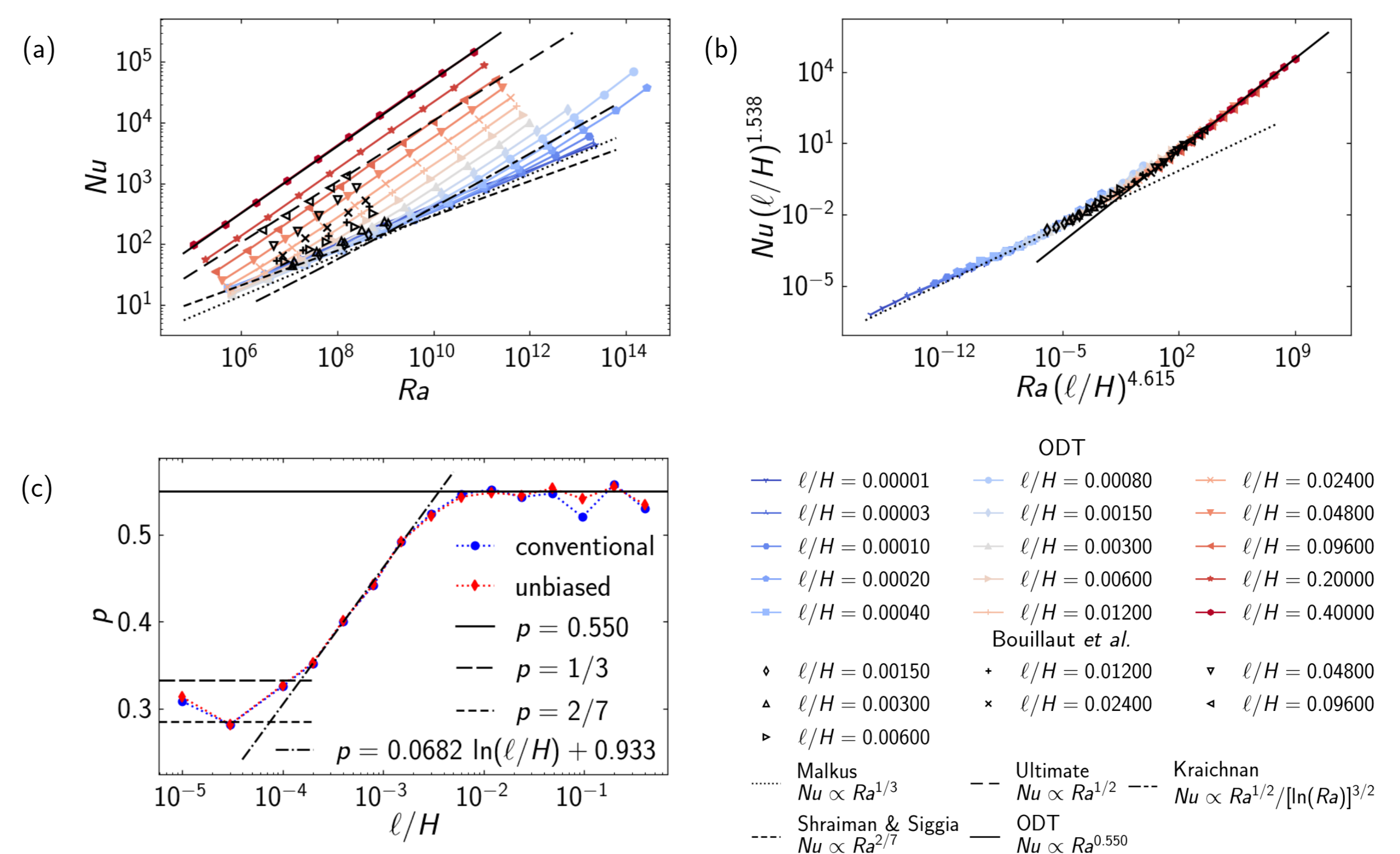


**Figure 3:** Scaling regimes of the heat transfer in turbulent thermal convection with internal sources/sinks at  $Pr = 1$ . (a)  $Ra$  number and  $\ell/H$  dependence of the  $Nu$  number. (b) Rescaled data collapses approximately. (c) Exponent  $p$  of high- $Ra$  effective scalings for various prescribed  $\ell/H$ .

## Conclusions

- **ODT** is a dimensionally reduced, **stochastic turbulence model** that aims to resolve wall-normal (vertical) transport processes on **all relevant scales** of the flow.
- **ODT reproduces and extrapolates** the reference experiments [9] with **fixed model parameters**.
- **ODT predicts a turbulent transition** from the classical ( $p \approx 0.3$ ) to the 'ultimate' regime with scaling exponent  $p \approx 0.55$ , which slightly exceeds the 'turbulence-only' upper bound  $p = 1/2$  but is well within  $p_{\text{max}} = 1$  [15].
- **ODT predicts a transitional range** involving **logarithmic dependence of  $p$  on  $\ell/H$**  that has *not* previously been observed or proposed.

## Forthcoming research

- $Pr$  number dependence of the  $Nu$  number
- Control parameter dependences of the Reynolds ( $Re$ ) number
- Assessment of upper bounds by variation of source term  $Q$

## References

- [1] F. Chillà, J. Schumacher, *Eur. Phys. J. E* **35**, 58 (2012).
- [2] S. Lepot, S. Aumaitre, B. Gallet, *PNAS* **115**, 8937 (2018).
- [3] K. K. Chandrakar, W. Cantrell, S. Krueger, R. A. Shaw, S. Wunsch, *J. Fluid Mech.* **884**, A19 (2019).
- [4] A. R. Kerstein, *J. Fluid Mech.* **392**, 277 (1999).
- [5] D. O. Lignell, A. R. Kerstein, G. Sun, E. I. Monson, *Theor. Comp. Fluid Dyn.* **27**, 273 (2013).
- [6] S. Wunsch, A. R. Kerstein, *J. Fluid Mech.* **528**, 173 (2005).
- [7] E. D. Gonzalez-Juez, A. R. Kerstein, D. O. Lignell, *J. Fluid Mech.* **677**, 218 (2011).
- [8] M. Klein, H. Schmidt, *Proc. 11th Int. Symp. Turb. Shear Flow Phen.* (Southampton, UK, 2019), vol. 1, pp. 1–6.
- [9] V. Bouillaut, S. Lepot, S. Aumaitre, B. Gallet, *J. Fluid Mech.* **861**, R5 (2019).
- [10] S. Grossmann, D. Lohse, *J. Fluid Mech.* **407**, 27 (2000).
- [11] W. V. R. Malkus, *Proc. Royal Soc. Lond. A* **225**, 185 (1954).
- [12] B. I. Shraiman, E. D. Siggia, *Phys. Rev. A* **42**, 3650 (1990).
- [13] E. A. Spiegel, *Asrophys. J.* **138**, 216 (1963).
- [14] F. H. Busse, *J. Fluid Mech.* **37**, 457 (1969).
- [15] B. Miquel, S. Lepot, V. Bouillaut, B. Gallet, *Phys. Rev. Fluids* **4**, 121501(R) (2019).